Journal of Nuclear Materials 393 (2009) 230–234

Contents lists available at ScienceDirect

Journal of Nuclear Materials

journal homepage: www.elsevier.com/locate/jnucmat

Experimental investigation of helium migration in an fcc aluminum matrix

Benny Glam [a,b,*], Daniel Moreno [a], Shalom Eliezer [a], Dan Eliezer [b]

[a] Soreq Nuclear Research Center, Yavne 81800, Israel
[b] Ben-Gurion University of the Negev, Beer-Sheva, Israel

ARTICLE INFO

Article history:
Received 31 March 2009
Accepted 4 June 2009

ABSTRACT

Experimental investigation of helium migration in an fcc aluminum is reported. A pure aluminum with 0.15 wt% of ^{10}B was neutron-irradiated to obtain $(1.2 \pm 0.2) \times 10^{24}\,m^{-3}$ helium atoms in the metal according to the reaction $^{10}B + n \rightarrow {}^{7}Li + {}^{4}He$. The post-irradiated metal was observed in situ in TEM while the sample was heated to 470 °C with a hot stage holder.

A helium-rich area was found in the vicinity of nanometric ^{10}B segregates that were not solute in the aluminum. The helium-rich area was characterized as a polygonal faceted region. According to EELS measurements, this area is saturated with $N_{He} = (3 \pm 1) \times 10^{28}\,m^{-3}$ helium atoms, which are (30–65)% of the atoms in the observed area.

It was found that the helium-rich area expands due to helium migration. Electron beam diffraction revealed that the preferred orientation of the helium atoms' migration is normal to plane $(0\bar{2}2)$. The results are consistent with models for helium atoms migration between interstitial sites for an fcc metal.

1. Introduction

Mechanical property deterioration by helium embrittlement is attributed to helium atom creation and bubble formation, particularly in metals at high homologous temperatures ($T > 0.5T_m$, where T_m is the melting temperature). [1].

Theoretical investigation of the atomistic behavior of helium-vacancy (He_nV_m, where He_n are n helium atoms and V_m are m voids) clusters was carried out analytically and by molecular dynamics codes during the last few decades [2–4]. Despite many years of research regarding helium's effects in metals there are still many unknowns, especially regarding the initial stages of voids and bubble nucleation.

One method to induce helium in metals is based on neutron irradiation of aluminum–boron samples [5,6]; this procedure was used in this work.

When the post-irradiated metal is heated, the helium atoms combine into clusters and into bubbles. Tiwari and Singh [7] investigated the effect of temperature on the final helium bubble radius in aluminum and copper. In order to see the migration process of helium and bubble formation, in situ observation during the heating is required.

In this report, we present an investigation of helium migration in an fcc aluminum using TEM. Micrograph images and respective electron beam diffraction on aluminum with ^{10}B after neutron irradiation during in situ heating using a hot stage holder are reported.

2. Alloy preparation

Pure aluminum (99.9999%) with 0.15 wt% ^{10}B powder was melted in an arc furnace. This amount of ^{10}B is solute in the aluminum at the elevated temperatures in the arc furnace. Since the solubility of ^{10}B in a solid Al is negligibly small [8], nanometric ^{10}B segregates were formed after solidification. The prepared metal was then neutron-irradiated in the Soreq nuclear reactor with a flux of $\phi = 3 \times 10^{17}$ $(n/m^2\,s)$ for 20 h. The concentration of helium atoms N_{He} that were created in the bulk of the sample from the reaction $^{10}B + n \rightarrow {}^{7}Li + {}^{4}He$ is given by $N_{He} = \phi\sigma N_{10_B} t = 1.2 \times 10^{24}$ (m^{-3}), where $\sigma = 4.0 \times 10^{-25}\,(m^2)$ is the cross-section of the ^{10}B atom, $N_{10_B} = 7.7 \times 10^{25}\,(m^{-3})$ is the number of ^{10}B atoms per unit volume, and $t = 20\,(h)$ is the irradiation time. The Li product at this small concentration is solute in the Al matrix and therefore can be neglected [9].

After irradiation, the Al–^{10}B alloy was rolled to a 2.7 mm thickness plate and TEM samples were prepared. The Al–^{10}B plate was cut with a low speed saw to obtain 500 μm thickness foils. Disks with a 3 mm diameter were punched from the foils and were thinned to 100 μm by grinding. Subsequently, the disks were thinned to a hole in their center by an electro-polishing jet in a Tenupol 50 device. The combined procedure of graded grinding and electro-polishing at low temperatures ensures a minimum influence of the preparation procedure on the specimen's microstructure. The estimated thickness of the observed region near

* Corresponding author. Address: Soreq Nuclear Research Center, Yavne 81800, Israel. Tel.: +972 8 943 4914, Mobile: +972 52 850 1508; fax: +972 8 943 4346.
E-mail addresses: glam@bgu.ac.il, benny.glam@gmail.com (B. Glam), dmoreno@netvision.net.il (D. Moreno), shalom.eliezer@gmail.com (S. Eliezer), dan.eliezer@gmail.com (D. Eliezer).

0022-3115/$ - see front matter © 2009 Elsevier B.V. All rights reserved.
doi:10.1016/j.jnucmat.2009.06.008

the hole, where the electron beam can be transmitted, is about 50–150 nm.

3. Experimental results

The observations were carried out in an FEI Titan model TEM with an acceleration of 300 keV. TEM images of selected areas of a specimen that had been heated to 470 °C are shown in Fig. 1a–f. A polygonal area with sharp boundaries was observed (Fig. 1a–e). A defocused image under magnification of this area revealed a formation of nanometric helium bubbles, as shown in Fig. 1f. The edge contrast arises because the helium displaces the aluminum reflecting planes. Similar contrast effect of stacking fault has been observed by TEM in metals [10]. The number of helium atoms in

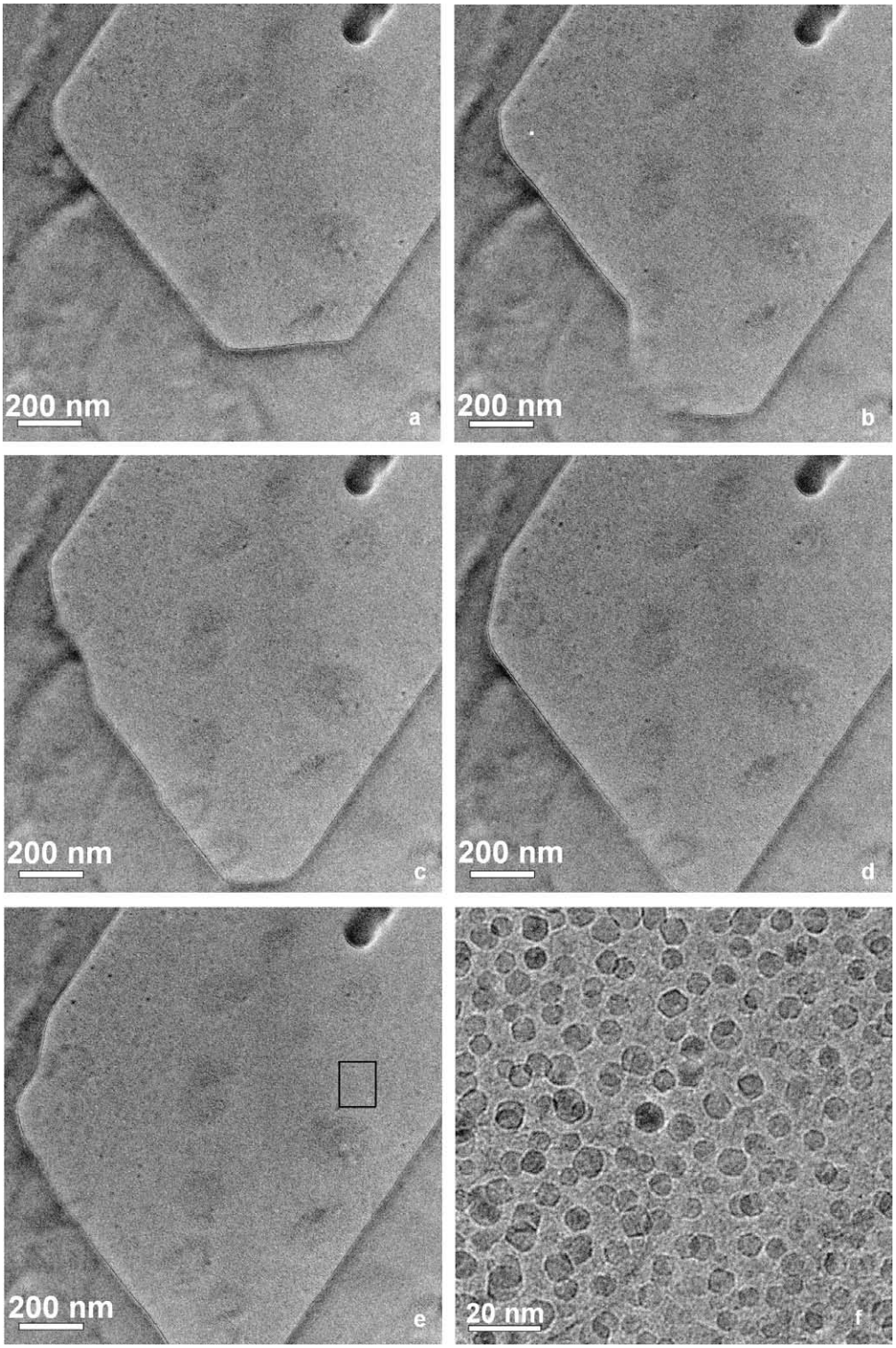

Fig. 1. TEM images of migration of the helium-rich area in aluminum during heating to 470 °C in the hot stage holder (a–e). A defocused image under magnification of this area revealed a formation of nanometric helium bubbles (f).

this area was measured with an electron energy loss spectrum (EELS) device. According to EELS measurement, the number of helium atoms is given by [11]:

$$N_{He} = \frac{I_k}{I_0} \cdot \frac{1}{\sigma_k} \cdot \frac{1}{d} \quad (1)$$

where I_k is the intensity of the electron loss spectrum at 21.5 eV (first helium ionization energy) and I_0 is the intensity of the unscattered electrons, $\sigma_k = 3 \times 10^{-23}$ m^2 is the electron cross-section of the appropriate scattered electrons, and $d = 70$ nm is the foil thickness in the TEM experiment. In the helium area there are $N_{He} = (3 \pm 1) \times 10^{28}$ m^{-3} helium atoms, which are (30–65)% of the atoms in the observed area. For comparison, the number of helium atoms in the rest of the aluminum matrix is $(1.2 \pm 0.2) \times 10^{24}$ m^{-3}, which is 20 appm.

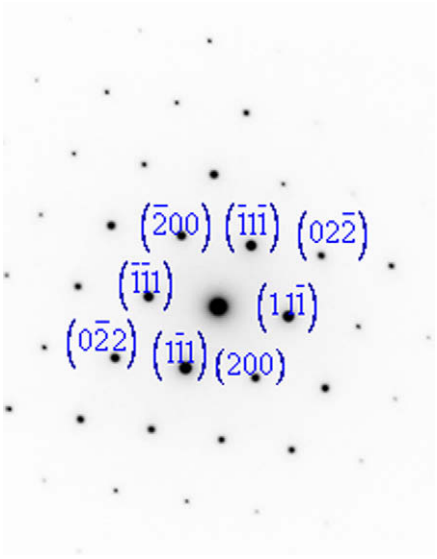

Fig. 2. Diffraction pattern of the selected area in Fig. 1.

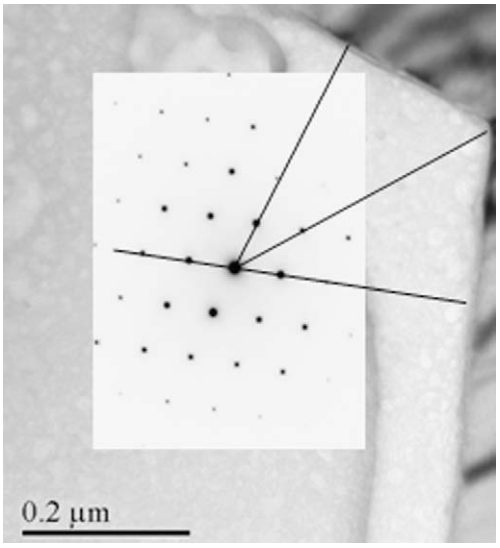

Fig. 3. TEM image with the diffraction pattern of the selected area after cooling to room temperature. The vectors to the diffraction spots indicate that the boundaries of the helium-rich areas are parallel to the aluminum crystallographic planes $(\bar{1}\,\bar{1}\,1)$, $(1\,\bar{1}\,1)$ and $(0\,\bar{2}\,2)$.

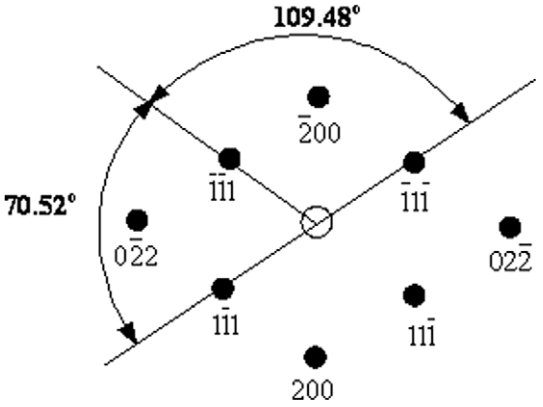

Fig. 4. Theoretical diffraction pattern in fcc metal with zone axis [0 1 1].

The formation of an area with a high concentration of helium is attributed due to the existence of 5 nm diameter segregated boron particles that were found in the vicinity of the polygonal area. During the neutron irradiation a high helium concentration region was formed around the boron particles according to the nuclear reaction $^{10}B + n \rightarrow {}^{7}Li + {}^{4}He$. At room temperature the diffusion rate of helium in the aluminum is very low. It increases exponentially with temperature [12]. The diffusion coefficient of helium atoms in aluminum at 470 °C is higher by two orders of magnitude than at room temperature, therefore helium atoms are moving fast in the metal until they are trapped in the lattice defects. The helium migration and bubble formation in these conditions continuously develop in minutes and can be observed by in situ TEM.

The images in Fig. 1a–e were taken at one second intervals from 1a to 1e. In Fig. 1b the helium area started to expand and the horizontal boundary at the bottom moved downwards. Although the diagonal boundary at the bottom seems to be also moving, Fig. 1c shows that this shape was preserved. The helium area continued to expand downward along a direction perpendicular to the lower boundary as shown in Fig. 1a–e. The expansion of the other boundaries is more moderate.

The sharp boundaries and the migration of the helium area in a preferred direction imply that this phenomenon is related to the aluminum crystallographic directions. A diffraction image was taken after cooling the specimen to room temperature, in order

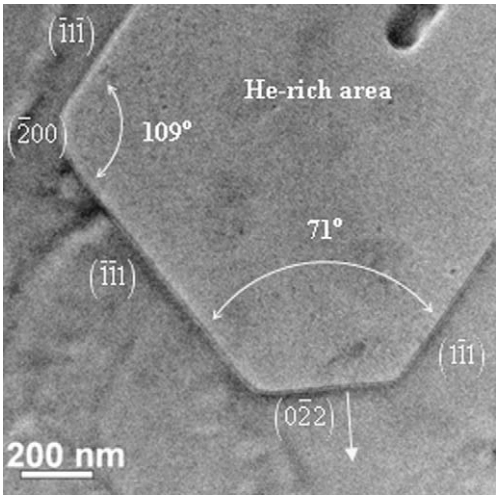

Fig. 5. TEM image of the helium-rich area in aluminum during heating to 470 °C. The angles between the boundaries reveal that the boundaries are parallel to the crystallographic planes.

Table 1
A comparison of the calculated angles between crystallographic planes in an fcc metal (Fig. 4) and the measured angles between the polygon sides (Fig. 5).

Between planes	Theoretical angle (°)	Measured angle in the TEM image (°)
$(1\bar{1}1)$ and $(\bar{1}\bar{1}1)$	70.52	71 ± 1
$(\bar{1}1\bar{1})$ and $(\bar{1}\bar{1}1)$	109.48	109 ± 1

to stop the helium migration and to stabilize the diagnosed area. The electron beam diffraction pattern and the relevant crystallographic planes notations are shown in Fig. 2. It was found that the zone axis lies along the [0 1 1] direction, hence the observed plane in the TEM is (0 1 1). The diffraction image combined with the TEM image of the observed area is shown in Fig. 3. One can see that the vectors to the spots reflected from planes $(\bar{1}\bar{1}1)$ and $(1\bar{1}1)$ in the diffraction image are perpendicular to the boundaries of the helium-rich area in the TEM image. The vector to plane $(0\bar{2}2)$ is pointing to the corner between the two boundaries. This is the preferred migration direction of the helium area. These results reveal that the boundaries of the helium area are parallel to the corresponding crystallographic planes of the aluminum bulk. Analysis of the angles between the diffraction spots supports these findings. A schematic description of the diffraction image as received in the experiment is shown in Fig. 4 [13]. A comparison of the calculated angles between crystallographic planes in an fcc metal as shown in Fig. 4, and the measured angles between the polygon sides in our experiment (Fig. 5) is given in Table 1. The agreement between the experimental and calculated angles indicates that the boundaries are parallel to the crystallographic planes as shown in Fig. 5. The arrow in Fig. 5 shows the migration direction of the lower boundary. It is parallel to the plane $(0\bar{2}2)$. The direction of the migration is normal to this plane.

4. Analysis and discussion

The experimental results show that helium migrates in the aluminum in a direction normal to the family of planes {1 1 1} and the plane $(0\bar{2}2)$. The expansion rate of the boundaries seems to be higher in the direction parallel to plane $(0\bar{2}2)$ than in the other directions. Helium bubbles are formed in the helium-rich area behind the migration front.

To understand this behavior it is essential to examine the helium–metal interaction. Past research in this field has found that helium atoms get into the interstitial sites and create clusters in the metal defects that become nucleation sites for the bubble formation [14]. It was also suggested that the helium atoms in the aluminum matrix increase the stability of vacancy clusters and act as a catalyst for the formation of He-void clusters [15,16].

Aluminum has an fcc atomic structure with two types of interstitial voids: the larger voids are known as octahedral sites and the smaller voids are known as tetrahedral sites [17]. In the fcc metal the octahedral interstitial site is the favorable position for interstitial helium. [15,16,18]. Ab initio calculations made by Yang et al. [15] showed that the migration energy of interstitial helium atoms between two octahedral sites without crossing the tetrahedral site is 0.16 eV, while passing via the tetrahedral site is 0.13 eV. Since the difference between tetrahedral and octahedral diffusion path is only 0.03 eV, the helium migration in our experiments at 470 °C (=0.064 eV) will be probably a combination of both types of transitions.

According to this model, and the behavior of the sample under the TEM, we suggest the following explanation. Due to neutron irradiation of a specimen containing nanometric boron segregates helium-rich regions are initially present in the sample. After irradiation the specimen was heated in the TEM and the diffusion rate of helium in the aluminum matrix is accelerated exponentially as a function of the temperature. The amount of helium that can be absorbed by a specific region of the material depends on the number of vacancies available. Therefore the helium migrates to areas that contain smaller proportion of helium atoms, as observed in the experiment.

The initial step of the helium migration is a jump between octahedral sites either directly or via tetrahedral sites. In our TEM experiments the observation direction is normal to the plane (0 1 1). While looking on this plane, the jump of helium atoms from the octahedral site at the center [2 2 2] to the next octahedral site, as shown by the arrows in Fig. 6, will appear as a migration of the helium front in a direction normal to plane $(0\bar{2}2)$. The other possible vacant octahedral sites that the helium atoms could jump into are not lying in the plane (0 1 1) and therefore the migration of helium in directions normal to planes {1 1 1} looks less dominant by our TEM two-dimensional observations.

This interpretation of helium atom migration in aluminum, based on helium-vacancy models is consistent with our TEM experiment as shown in Fig. 1a–e.

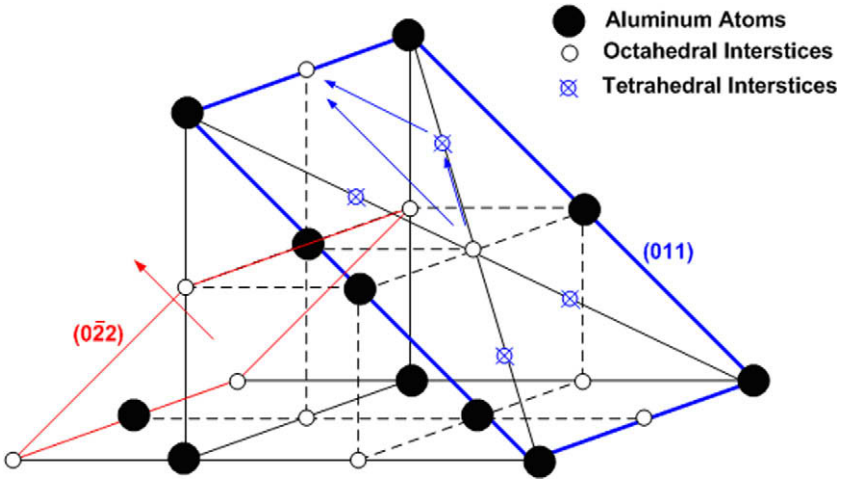

Fig. 6. A schematic fcc lattice with jump paths between two octahedral sites.

5. Conclusions

Migration of helium in aluminum was observed in situ by TEM with a hot stage holder while heating the metal. The TEM observation and calculation of the number of helium atoms from EELS revealed a helium-rich area in the vicinity of boron segregates. During the specimen heating, the helium starts to migrate to other areas and the helium-rich area expands. Electron beam diffraction reveals that the migration direction is normal to the planes $(0\bar{2}2)$ and {1 1 1} while the observed direction is normal to plane (0 1 1). These findings can be explained by the migration of helium atoms in an fcc aluminum lattice through interstitial sites.

Acknowledgements

The authors would like to thank Dr. Michael Aizenshtein for his metallurgical help and Dr. Vladimir Ezesky for mastering the TEM and the contributing discussions. This work was supported by the joint VATAT-IAEC common lab foundation.

References

[1] H. Trinkaus, B.N. Singh, J. Nucl. Mater. 323 (2003) 229–242.
[2] J.B. Adams, W.G. Wolfer, J. Nucl. Mater. 166 (1989) 235–242.
[3] K. Morishita, R. Sugano, B.D. Wirth, J. Nucl. Mater. 323 (2003) 243–250.
[4] K. Morishita, R. Sugano, B.D. Wirth, Nucl. Instrum. Methods B 202 (2003) 76–81.
[5] S.R. Pati, P. Barrad, J. Nucl. Mater. 31 (1969) 117.
[6] B. Glam, S. Eliezer, D. Moreno, D. Eliezer, J. Nucl. Mater. 2009, doi:10.1016/j.jnucmat.2009.03.057.
[7] G.P. Tiwari, J. Singh, J. Nucl. Mater. 172 (1990) 114–122.
[8] P.M. Hansen, Constitution of Binary Alloys, second ed., McGraw-Hill, New York, 1958.
[9] S.K. Nowak, J. Met. (1956) 553–556.
[10] R.E. Smallman, R.J. Bishop, Modern Physical Metallurgy and Materials Engineering, sixth ed., Butterworth Heinemann, Oxford, 1999.
[11] R.F. Egetron, Ultramicroscopy 3 (1978) 243–251.
[12] H.R. Glyde, K.L. Mayne, J. Nucl. Mater. 15 (1965) 997.
[13] J.W. Edington, Practical Electron Microscopy in Materials Science, Van Nostrand Reinhold Co., New York, 1991.
[14] D.J. Reed, Rad. Eff. 31 (1977) 129–147.
[15] L. Yang, X.T. Zu, F. Gao, Physica B 403 (2008) 2719–2724.
[16] B.Y. Ao, J.Y. Yang, X.L. Wang, W.Y. Hu, J. Nucl. Mater. 350 (2006) 83–88.
[17] C. Barrett, T.B. Massalski, Structure of Metals, Pergamon Press, Oxford, 1982.
[18] B.B. Nielsen, A.V. Veen, J. Phys.: Mater. Phys. 15 (1985) 2409–2420.